Study on Optical Devices Based on Single-Polarization Photonic Crystal Fiber

Zejun ZHANG*

I. INTRODUCTION

In the last four decades, telecommunication industry and sensing technology has been revolutionized with the development of optical fiber technology. Compare with the traditional telecommunication systems, optical communication systems are famous for their high-speed and large-capacity transmission capabilities. With the continuous development of optical fibers and high-performance optical devices as well as the multiplexing communication systems, the IoT (Internet of things) society has been further realized, which makes our daily life more convenient.

In recent years, many new types of fibers have been designed and fabricated for optic telecommunication and sensing applications. Photonic crystal fiber (PCF)[1],[2], is a new technology that paves the way in optical communication due to its flexible structure and the special properties. According to the different light wave guided mechanisms, PCF can be generally divided into two categories: the holey fiber (HF) that light wave confinement using total internal reflection at the core-cladding boundary; another kind of PCF is called photonic band-gap (PBG) fiber that light is confined by the photonic band-gap which is generated by setting a periodic structure in the cladding region. In comparison to conventional optical fiber, PCF shows basic properties like large birefringence, non-linearity and single polarization property that can be tailored to achieve extraordinary outputs[2]. One of these properties is the absolutely single polarization transmission and a number of single-polarized PCF structures have been proposed[3]-[10]. Utilizing an asymmetric core or cladding distribution that caused by adjusting the arrangement or shapes of the air holes, large birefringence can be obtained, and the single-polarization property can be easily realized. In 2007, elliptical-hole core circular-hole holey fiber (EC-CHF), a novel single-polarized holey fiber with a core consisting of elliptical-holes, has been proposed for achieving the single polarization transmission easily[6]. Simulation results illustrate that an EC-CHF can be easily designed to transmit only the *x*- or *y*-polarization by changing the major axis direction of the elliptical-holes in core region. Moreover, a PBG fiber with elliptical-hole lattice core has also been proposed that can achieve single polarization with a wide bandwidth of 420nm[10]. So far, we can see that the single-polarization PCFs have been widely studied.

Multiplexing communication systems can effectively improve the information transmission capacity, such as time division multiplexing (TDM), frequency division multiplexing (FDM), polarization division multiplexing (PDM), *etc*. Several polarizing optical devices play an indispensable role in PDM system and optical-fiber sensing system. Among polarizing optical devices, polarization splitter (PS), which can split a light beam into two orthogonal polarization states, is very important component in coherent optical communication system. In 2003, a PS with dual-core PCF has been proposed by Zhang and Yang[11]. An extinction ratio (ER) of -11 dB and a bandwidth of 80 nm can be achieved in this PS. After that, several kinds of PSs based on new structure of PCFs were proposed[12]-[17]. In 2004, Saitoh *etal*. proposed a PS using three-core PCF, which has an ER better than -20 dB and a bandwidth of 37 nm with a device length of 1.9 mm[12]. In 2013, Lu *etal*. proposed a PS based on three-core PCF which has an ER as low as -20 dB and a bandwidth of 400 nm[17]. However, this splitter has long coupling lengths of *x*- and *y*-polarization modes, and there is a quite large difference between the two kinds of coupling lengths. This makes the design of PS become complicated. Although many new kinds of PSs based on PCF have been proposed, none of them can realize the cross-talk-free separation.

My research is mainly focus on the design of high-performance polarizing optical devices which have a great application potential in the future. In this paper, I will mainly introduce a cross-talk free PS based on the single-polarized EC-CHFs. In part II, I will briefly explain the coupled mode theory that I used in this design. A design example of cross-talk free PS is given in part III, including the geometric parameters, the light propagation characteristic and the structural tolerance. Finally, the conclusion and future works.

II. PRINCIPLE OF CROSS-TALK FREE PS

In this section, I will briefly introduce the design principle of a cross-talk free PS. In recent decades, most studies on PSs based on PCF have a multi-core distribution and achieve the polarization splitting by using the coupling length difference between *x*- and *y*-polarizations. However, for this kind of PSs, it is necessary to discuss their extinction ratio (ER). While for the proposed PS in my research, it consists with three PCFs in parallel, as shown in Fig. 1. An polarization independent holey fiber in the middle as the input waveguide, and two single-polarized PCFs at both sides as two output waveguides. When the phase matching condition between three waveguides are perfectly satisfied, then an arbitrary polarized incident light will be completely separated into two orthogonal polarized compo-nents and coupled into their corresponding single-polarization PCF. Even if the phase matching condition can not be perfectly satisfied, the uncoupled polarization component will remain in the middle waveguide, while for the output waveguides, there is still only one polarization exists. Therefore, the ER for each output waveguide is 0, and the cross-talk free property is

Zejun ZHANG（張 沢君）* 助教　電気電子情報工学科
Assistant Professor, Dept. of Electrical, Electronics, and Information Engineering

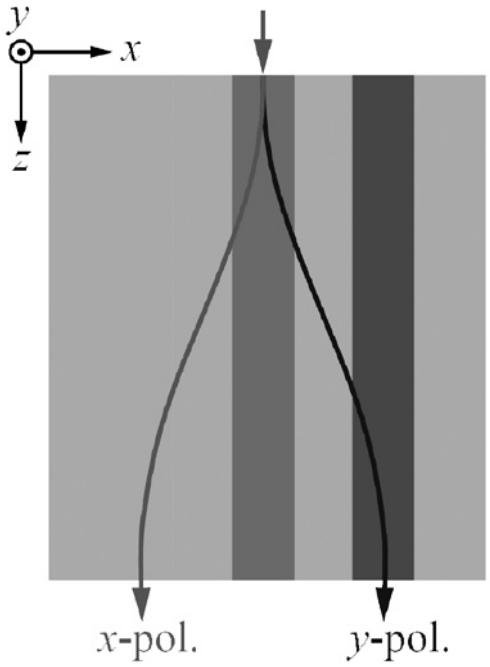

Fig. 1. Schematic of a cross-talk free PS with three PCFs in parallel.

achieved.

Since the polarization splitting are independent to each other, then the mode coupling can be analyzed independently. Such as for x-polarization splitting, it is necessary to only consider the analysis between input waveguide and only x-polarized output waveguide. According to the coupled mode theory, the mode coupling equation two waveguides (waveguide a and b)is given as follows,

$$\frac{d}{dz}\begin{pmatrix}\Phi_1\\ \Phi_2\end{pmatrix} = -\mathrm{i}\begin{pmatrix}\beta_a & \kappa_{ab}\\ \kappa_{ba} & \beta_b\end{pmatrix}\begin{pmatrix}\Phi_1\\ \Phi_2\end{pmatrix} \tag{1}$$

where β_a and β_b are the propagation constants of two isolated waveguides, and κ_{ab} and κ_{ba} represent the coupling coefficients between two waveguides. Based on the coupling equation, we note that coupling length L_c can be calculated by

$$L_c = \frac{0.5\lambda}{n_{\mathrm{eff,e}} - n_{\mathrm{eff,o}}} \tag{2}$$

where λ is the operation wavelength, $n_{\mathrm{eff,e}}$ and $n_{\mathrm{eff,o}}$ are the effective indices of the even and odd modes for *x*-polarization or *y*-polarization. In a coupled system, the coupling efficiency F between the two adjacent waveguides is defined as

$$F = 1 - \left(\frac{n_{\mathrm{eff},1} - n_{\mathrm{eff},2}}{n_{\mathrm{eff,e}} - n_{\mathrm{eff,o}}}\right)^2 \tag{3}$$

In order to design the PS, all the coupled modes and isolated modes are calculated by FV-FEM in this paper.

After explain the design principle of cross-talk free PS, I will briefly introduce the single-polarized EC-CHF[7]. For a conventional PCF, whose cladding region is consisted by periodic air holes and the core region is formed by defecting an air hole, the structure is isotropic, and both *x* and *y*-polarization can be propagated. However, EC-CHFs which have elliptical air holes in the core region to destroy symmetry can achieve single-

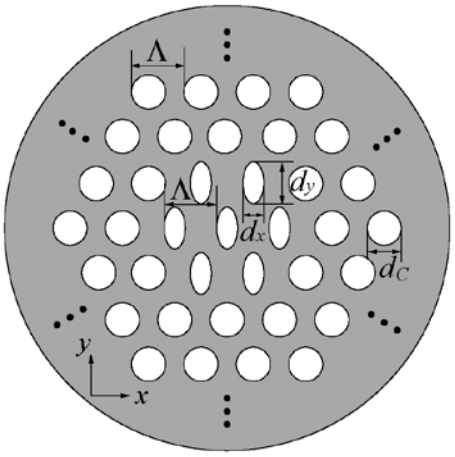

Fig. 2. Cross-section view of a *y*EC-CHF[7].

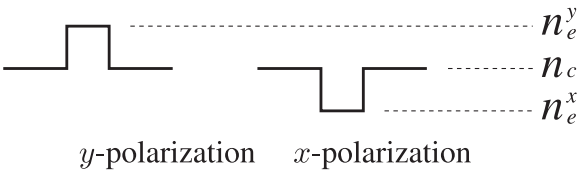

Fig. 3. Equivalent refractive index distribution in the radial direction through the core center of a *y*EC-CHF.

polarization property easily. A cross-section view of an EC-CHF with one-ring elliptical hole core whose major axis is aligned along the *y* direction is indicated in Fig. 2. When the circular holes of the cladding are isotropic, the birefringence only in the core region can be achieved by introducing elliptical-holes in the core region, and the absolutely single polarization transmission also can be realized with appropriate air hole parameters. If $d_x<d_y$, the fiber will be a *y*EC-CHF that transmits only the *y*-polarized wave. Fig. 3 shows the equivalent refractive index distribution for the *x*- and *y*-polarizations in the radial direction through the core center of a *y*EC-CHF, respectively. For the *y*-polarized wave, compared with the cladding region, the core region has higher effective refractive index of fundamental space-filling mode (FSM). On the other hand, for the *x*-polarized wave, the core region has the lower effective refractive index of FSM. Therefore, the single-polarization transmission can be achieved. If $d_x>d_y$ by exchanging the directions of the major and minor axes of the elliptical-holes, only the *x*-polarized wave can be transmitted. This kind of EC-CHF is referred to as an *x*EC-CHF. In addition, if $d_x=d_y<d_C$, both of the *x* and *y*-polarized waves can be transmitted simultaneously and we refer to it as a circular-hole core circular-hole holey fiber (CC-CHF) in this research.

III. DESIGN OF PS BASED ON EC-CHF

In this section, referring my paper[18] and[19], I will briefly introduce my research through two design examples of PSs based on large hole and small hole EC-CHFs, respectively.

A. Design of PS With Large Hole EC-CHFs

Firstly, I will give the design examples of PS with large hole EC-CHFs (air filling fraction in core is 36.7%)[18]. In practical design, in order to

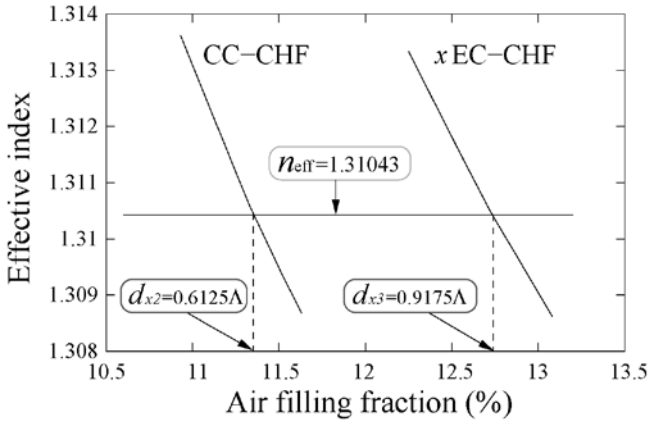

Fig. 4. Effective refractive indices n_{eff} of the CC−CHF and xEC−CHF as a function of the air filling fraction[18].

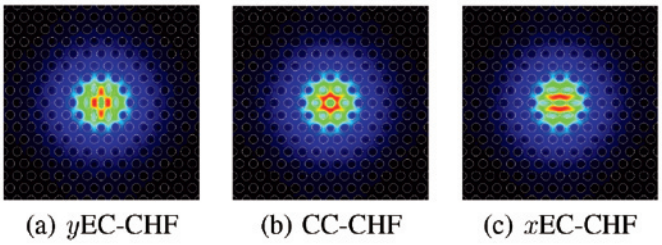

Fig. 5. Magnetic field distributions for three phase matching EC−CHFs.

reduce the insertion loss, it is necessary to satisfy the phase matching condition based on the coupled mode theory. In this study, the parameters of the reference waveguide yEC-CHF are set as follows: the lattice pitch is Λ= 1.24 μm, the refractive indices of background material silica and air holes are n_1=1.45 and n_2=1, respectively, the operating wavelength is λ=1.55 μm, the cladding hole size is d_C=0.65Λ , the major axis diameter is d_{y1}=0.9 Λ , and the ellipticity is d_{y1}/d_{x1}=2. Under such conditions, the air hole sizes in the core region of the CC-CHF and xEC-CHF are determined by meeting the phase matching condition with the reference waveguide yEC-CHF. Figure 4 shows the effective refractive indices n_{eff} of the CC-CHF and xEC-CHF as a function of air filling fraction. The blue line represents the effective refractive index of the yEC-CHF. The phase matching core hole sizes are d_{x2}=0.6125Λ for the CC-CHF, and corresponds to d_{x3}=0.9175Λ for the xEC-CHF. The magnetic field distributions for each EC-CHF are shown in Figure 5. The mode field diameter for each structure is almost the same.

After we determined the hole sizes of each waveguide, the mode couplings of x- and y-polarization have also been discussed. Here, we set the core distance is 2Λ , and the super mode (even or odd modes) field distributions of each polarization are illustrated in Fig. 6 and 7, respectively. The calculated coupling lengths are L_x=638 μm and L_y=622 μm. In this research the average length has been adopted and the device length is set to L=630 μm. Normalized power along propagation distance of input and output waveguides are given in Fig. 8. Assuming that a 45-degree polarized light is incident on the CC-CHF, there is a slight deviation in the graph of the xEC-CHF and yEC-CHF according to the dif-ference of the coupling length. However, the normalized power at 630 μm of each wavguide is about

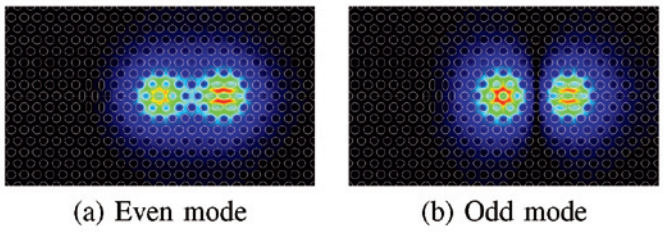

Fig. 6. Super mode field distributions of the x−polarization.

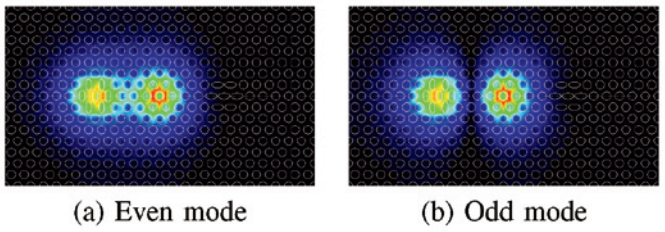

Fig. 7. Super mode field distributions of the y−polarization.

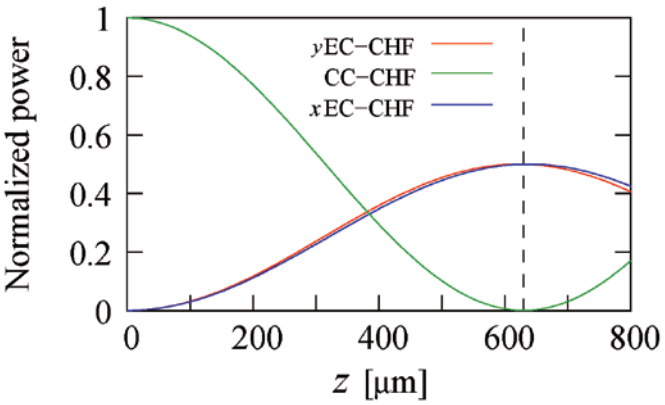

Fig. 8. Normalized power along the propagation distance[18].

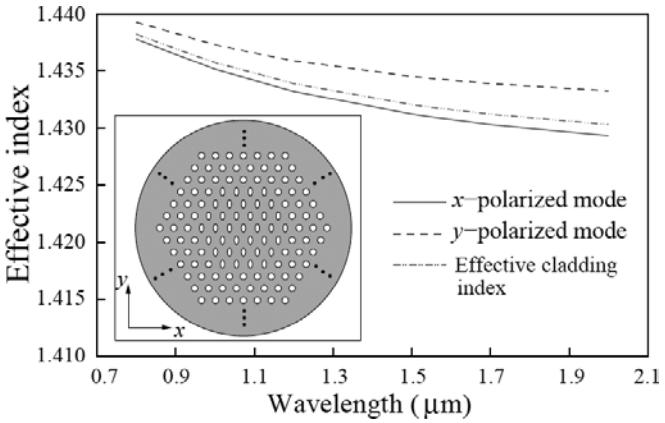

Fig. 9. Modal effective indices of x− and y−polarized modes and cladding effective index of a small hole yEC−CHF as a function of wave−length; the inset is a cross view of a 3−ring core small hole yEC−CHF.

49.98%, the loss due to the difference of the cou-pling length is almost negligible.

B. Design of PS With Small Hole EC-CHFs

After we designed the PS with the large hole EC-CHFs which have a

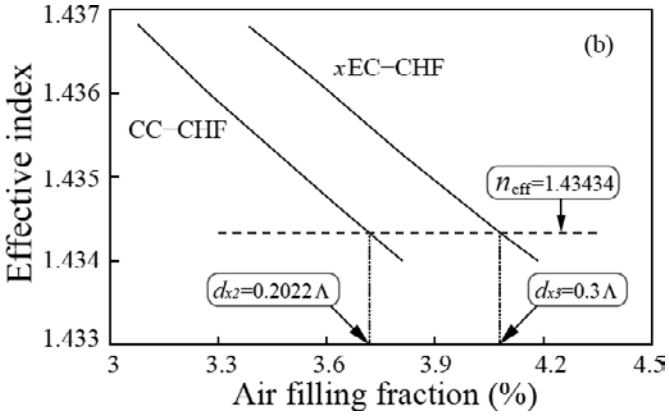

Fig. 10. Effective indices of the FSM in core region of the CC−CHF and *x*EC−CHF as a function of the air filling fraction[19].

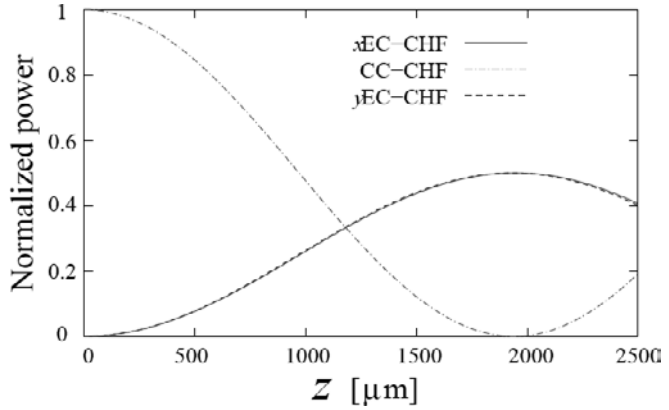

Fig. 11. Normalized power along the PS with the small hole EC−CHFs[19].

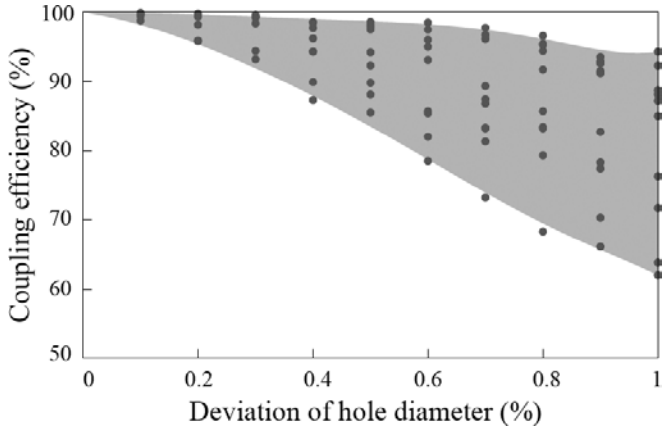

Fig. 12. Coupling efficiencies of the PS with the large hole EC−CHFs against the random deviation of all the air holes[19].

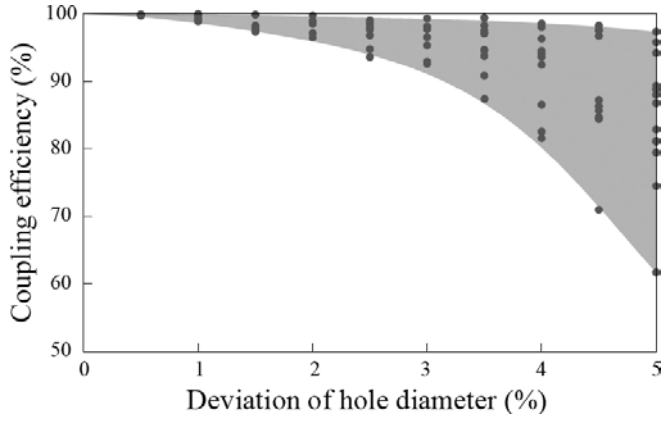

Fig. 13. Coupling efficiencies of the PS with the small hole EC−CHFs against the random deviation of all the air holes[19].

strong optical confinement of the waveguide, in order to obtain a Gaussian like mode field distribution which can improve the connectivity between the EC-CHF and a standard SMF, we designed the PS with small hole EC-CHFs[19]. The parameters of *y*EC-CHF are set as follows: d_{y1}＝0.3Λ for the major axis of elliptical holes, circular holes in cladding is d_c＝0.22Λ . The cross section of the small hole *y*EC-CHF is shown in the inset of Fig. 9, it can be seen that the fiber includes three rings of elliptical holes in the core region to increase the optical confinement since the EC-CHF is weakly guiding waveguide with the small holes. The modal effective indices of the two orthogonal polarization and the cladding effective index of the *y*EC-CHF as a function of wavelength are also shown in Fig. 9. From 0.8 μm to 2 μm, only *y*-polarized mode can be guided well in the fiber core because its modal effective index is obviously higher than the cladding effective index, whereas the *x*-polarized mode is lower than the cladding effective index.

Since EC-CHF with small holes has much more air holes than that with large holes, in order to reduce the calculation cost, here we meet the match the phase condition of each EC-CHF by calculating only the FSM of core region. Fig. 10 illustrates the vary of effective indices for the CC-CHF and *x*EC-CHF as a function of air filling fraction by the two design methods mentioned above. The phase matched holes in the core region for each waveguide are d_{x2}＝0.2022Λ for the CC-CHF and d_{x3}＝0.3Λ for the *x*EC-CHF. The distance between two adjacent core region is set to 3Λ and the estimated coupling lengths for *x*- and *y*-polarization are L_x＝1947 μm and L_x＝1933 μm, respectively. The de-vice length is set to L＝1940 μm.

The normalized power against propagation distance is illustrated in Fig. 11. The power of incident light in CC-CHF is almost 0 at 1940 μm, and *x*-polarized wave, *y*-polarized wave can be completely divided.

IV. TOLERANCE AND WAVELENGTH DEPENDENCE OF PS

Considering the current fabrication technology of PCF, the biggest problem in the fabrication process of EC-CHFs is the deviation of the circular or elliptical air holes away from the initial parameter values. So we discussed the effect of the deviation of the geometric parameters designed with the large and small hole EC-CHFs. Since the air holes deviate irregularly in fabrication, we investigated the coupling efficiency of the PS against all air holes varies randomly from the initial parameters. The parameters of each large hole EC-CHF are set to be as follows which can split light into two orthogonal states completely: d_{y1}＝0.9Λ for the *y*EC-CHF, d_{x2}＝0.6126Λ for the CC-CHF, d_{x3}＝0.9174Λ for the *x*EC-CHF, the ellipticity is d_{major}/d_{minor}＝2, d_C＝0.65Λ for the holes in cladding, each core is separated from the adjacent cores by two air holes, and the device length is fixed to 630 μm. Fig. 12 shows the coupling efficiency of the PS with the large hole EC-CHFs against the random deviation of all the air holes. It can be observed that the coupling efficiency is almost 90% when the deviation is smaller than 0.4% of their initial parameters, and the coupling efficiency is better than 60% when the deviation is smaller than 1% of the initial parameters. On the other

TABLE I PS WITH LARGE EC-CHF: COUPLING EFFICIENCY VERSUS THE DEVIATION FOR DIFFERENT PARTS OF THE DEVICE PARAMETERS AT EACH DEVIATION LEVEL

Deviation level	Core region			Cladding region
	xEC-CHF	CC-CHF	yEC-CHF	
-0.3%	88.9%	85.4%	87.6%	99.8%
-0.2%	94.5%	92.6%	94.3%	99.7%
-0.1%	97.9%	97.2%	98.4%	99.3%
0	99.9%	99.9%	99.9%	99.9%
0.1%	97.8%	98.0%	98.2%	98.6%
0.2%	94.3%	94.2%	94.0%	98.0%
0.3%	88.9%	88.0%	87.6%	97.3%

TABLE II PS WITH SMALL EC-CHF: COUPLING EFFICIENCY VERSUS THE DEVIATION FOR DIFFERENT PARTS OF THE DEVICE PARAMETERS AT EACH DEVIATION LEVEL

Deviation level	Core region			Cladding region
	xEC-CHF	CC-CHF	yEC-CHF	
-1%	86.1%	86.0%	86.3%	99.8%
-0.66%	94.0%	93.6%	94.1%	99.9%
-0.33%	98.6%	98.3%	98.6%	99.9%
0	100%	100%	100 %	100%
0.33%	98.3%	98.7%	98.4%	99.9%
0.66%	94.0%	94.9%	94.2%	99.9%
1%	87.7%	88.9%	87.8%	99.8%

hand, Fig. 13 shows the coupling efficiency of the PS with the small hole EC-CHFs designed in section 3 against the random deviation of all the air holes. Compared with the condition in Fig. 12, the coupling efficiency is better than 90% when the deviation is smaller than 3% of their initial parameters, and the coupling efficiency is better than 60% when the deviation is smaller than 5% of the initial parameters. The PS with the small hole EC-CHFs has a higher tolerance than the splitter with the large hole EC-CHFs because it has more elliptical air holes in core region which lead to reducing the average of deviation and decrease the impact to effective index of the waveguide.

Moreover, we have also examined the coupling efficiency versus the deviation for the respective hole sizes of each region, as shown in Table I and Table II. Here, all the hole sizes of the deviation part are varied with the same extent, such as if only the holes in xEC-CHF core region are expanded 1%, the coupling efficiency of the PS with small hole EC-CHFs will decrease to 87.7%. Compared with the random deviation of all the holes mentioned above, the deviation for one part of the device with same extent leads to worse coupling efficiency. It can be observed that the coupling efficiency with deviation in the core regions is much worse than the varies in the cladding, that is because in a EC-CHF, the effective index is sensitive to the hole sizes in the core region. So if we design this type of PS using other kinds of single-polarized PCFs[3]-[10] which have less holes or no holes in the core region, it may be possible to obtain a device with larger tolerance.

In addition, the splice loss between an EC-CHF and a SMF should also been considered, according to[22], the splice loss is not so large by adjusting the paramaters of EC-CHF and SMF.

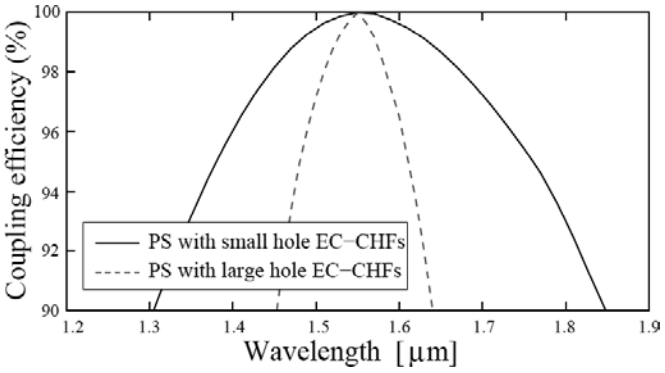

Fig. 14. Coupling efficiency of the PS versus the light wavelength[19].

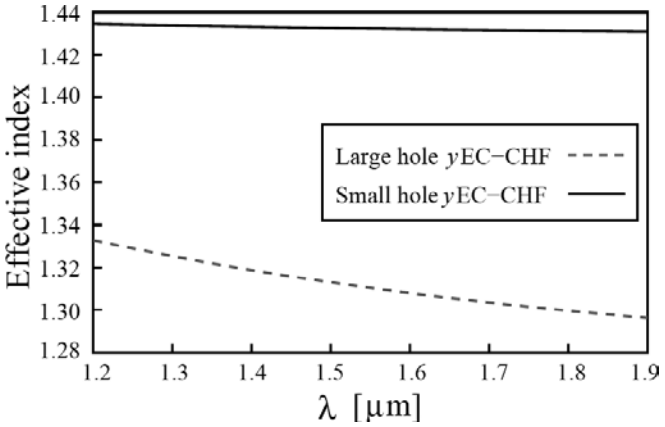

Fig. 15. Effective index of the yEC−CHF versus wavelength[19].

In order to achieve the wide-band transmission, we have also investigated the wavelength dependence of the PS with the large and small hole EC-CHFs, respectively, as shown in Fig. 14. The proposed PS with the large hole EC-CHFs has a coupling efficiency better than 20 dB at 1.55μm and a bandwidth of 50 nm from 1.52 to 1.57 μm, the PS with the small hole EC-CHFs exhibits a wider bandwidth of 160 nm from 1.47 to 1.63 μm. That is because the EC-CHF with small holes is a weakly guiding, and the effective index of the waveguide varies slightly versus wavelength, as shown in Fig. 15. So the proposed small hole PS has a wider bandwidth.

V. CONCLUSION

In this paper, we designed a novel PS using the single-polarized EC-CHFs which can divide the incident light into two orthogonal states completely without any cross-talk. We employed two methods to satisfy the phase matching condition between three waveguides, i.e., the effective index of each isolated waveguide and the only FSM of core region. Finally, the tol-erance and wavelength dependence of our designed two PSs with the large hole EC-CHFs and small hole EC-CHFs have also been investigated, re-spectively.

REFERENCES

[1] J. C. Knight, T. A. Birks, P. St. J. Russell, and D. M. Atkin, All-silica sin-gle-mode optical fiber with photonic crystal cladding, Optics Letters, 21(19), 1547-1549 (1996).

［2］P. St. J. Russell, Photonic-crystal fibers, Journal of Lightwave Technology, 24(12), 4729-4749 (2006).

［3］K. Satioh and M. Koshiba, Single-polarization single-mode photonic crystal fibers, IEEE Photonic Technology Letters, 15(10), 1384-1386 (2003).

［4］J. R. Folkenberg, M. D. Nielsen, and C. Jakobsen, Broadband single-polarization photonic crystal fiber, Optics Letters, 30(12), 1446-1448 (2005).

［5］F. Zhang, M. Zhang, X. Liu, and P. Ye, Design of wideband single- polarization single-mode photonic crystal fiber, Journal of Lightwave Technol-ogy, 25(5), 1184-1189 (2007).

［6］M. Eguchi and Y. Tsuji, Single-mode single-polarization holey fiber using anisotropic fundamental space-filling mode, Optics Letters, 32(5), 2112- 2114 (2007).

［7］M. Eguchi and Y. Tsuji, Design of single-polarization elliptical-hole core circular-hole holey fibers with zero dispersion at 1.55 μm, Journal of the Optical Society of America B, 25(10), 1690-1701 (2008).

［8］D. Hu, P. Shum, C. Lu, X. Yu, G. Wang, and G. Ren, Holey fiber design for single-polarization single-mode guidance, Applied Optics, 48(20), 4038-4043 (2009).

［9］R. Goto, S. D. Jackson, and K. Takenaga, Single-polarization operation in birefringent all-solid hybrid microstructured fiber with additional stress applying parts, Optics Letters, 34(20), 3119-3121 (2009).

［10］M. Eguchi, and Y. Tsuji, Single-polarization elliptical-hole lattice core photonic-bandgap fiber, Journal of Ligthwave Technology, 31(1), 177-182 (2013).

［11］L. Zhang and C. Yang, Polarization splitter based on photonic crystal fibers, Optical Express, 11(9), 1015-1020 (2003).

［12］K. Saitoh, Y. Sato and M. Koshiba, Polarization splitter in three-core photonic crystal fibers, Optical Express, 12(17), 3940-3946 (2004).

［13］L. Zhang and C. Yang, A novel polarization splitter based on the photonic crystal fiber with nonidentical dual cores, IEEE Photonic Technology Letters, 16(7), 1670-1672 (2004).

［14］L. Zhang and C. Yang, Polarization-dependent coupling in twin-core photonic crystal fibers, Journal of Ligthwave Technology, 22(5), 1367-1373 (2004).

［15］L. Zhang, C. Yang, C. Yu, T. Luo and A. E. Willner, PCF-based polarization splitters with simplified structures, Journal of Lightwave Technology, 23(11), 3558-3565 (2005).

［16］M. Chen, B. Sun, Y. Zhang and X. Fu, Design of broadband polarization splitter based on partial coupling in square-lattice phtotnic-crystal fiber, Applied Optics, 49(16), 3042-3048 (2010).

［17］W. Lu, S. Lou, X. Wang, L. Wang and R. Feng, Ultrabroadband polarization splitter based on three-core photonic crystal fibers, Applied Optics, 52(3), 449-455 (2013).

［18］Z. Zhang, Y. Tsuji, and M. Eguchi, Design of polarization splitter with single-polarized elliptical-hole core circular-hole holey fibers, IEEE Photonic Technology Letter, 26(6), 541-543 (2014).

［19］Z. Zhang, Y. Tsuji, and M. Eguchi, Study on crosstalk-free polarization splitter with elliptical-hole core circular-hole holey fibers, Journal of Light-wave Technology, 32(23), 3956-3962 (2014).

［20］M. Koshiba and Y. Tsuji, Curvilinear hybrid edge/nodal elements with triangular shape for guidedwave problems, Journal of Ligthwave Technology, 18(5), 737-743 (2000).

［21］Y. Tsuji and M. Koshiba, Adaptive mesh generation for full-vectorial guided-mode and beam propagation solutions, IEEE Journal of Selected Topics in Quantum Electronics, 6(1), 163-169 (2000).

［22］M. Eguchi and Y. Tsuji, Influence of reflected radiation waves caused by large mode field and large refractive index mismatches on splice loss evaluation between elliptical-hole lattice core holey fibers and conventional fibers, Journal of the Optical Society of America B, 30(2), 410-420 (2013).